Surface Oxidation Properties of Solution-Annealed Alloys 600 and 690 Depending on the Surface Conditions

Dong Woog Ha [a*], Yun Soo Lim [a], Dong Jin Kim [a], Chang Yeol Jeong [b]

[a] *Nuclear Material Research Division, Korea Atomic Energy Research Institute,*
Daedeok-Daero 989-111, Yuseong-Gu, Daejeon, Korea, 34057
[b] *Dept. of Nuclear and Energy System Engineering, Dongguk University,*
123, Dongdae-ro, Gyeongju-si, 38066, Korea
[*]*Corresponding author: hdu9270@kaeri.re.kr*

1. Introduction

Ni-based Alloy 600, which has been used widely for structural components in nuclear power plants, is known to be highly susceptible to primary water stress corrosion crack (PWSCC) in the primary water environments of a pressurized water reactor (PWR) [1]. Therefore, alloy 690 with a higher Cr content has become a substitute for alloy 600 due to the excellent corrosion resistance. However, alloy 690 has also been shown to be susceptible to PWSCC. The surface oxidation behavior affects an important aspect of the PWSCC initiation process [2]. The surface finish is also an important factor influencing the oxidation behavior of an alloy. According to Perez et al. [3], the surface finish produces a subsurface deformation layer with a high dislocation density, phase transformation and recrystallization, which would influence on affect oxidation behavior. In general, studies in laboratories using ground or polished specimens revealed the effects of the surface finish on the corrosion resistance properties [4]. The objective of the present study is to analyze the surface oxidation properties of solution-annealed alloys 600 and 690 depending on the surface conditions. Immersion tests were conducted in a simulated PWR primary water environment at 325 ℃ for 10 and 100 hours. The oxidized specimens were precisely characterized using an optical microscope and a scanning electron microscope (SEM).

2. Experimental procedures

2.1 Materials and Specimen Preparation

The materials used in this study were taken from round bars of mill-annealed alloys 600 and 690. Their compositions are shown in Table 1. In order to minimize the extent of carbide precipitation and to homogenize the compositional distribution, the alloy 600 and 690 samples were solution-annealed in air at 1150 ℃ for 1 hours and for 20 minutes, respectively, after which they were quenched in water. Specimens with dimensions of $8\times8\times1$ mm^3 were prepared from the alloys for an immersion test. The specimens were divided chemical polishing. Grinding was mechanically ground with waterproof abrasive paper up to 400 grit, polishing was mechanically ground to 2000 grit and then polished using 0.3 μm alumina powders. And chemical polishing was conducted in a 2 % bromine + 98 % methanol solution for 15 sec after polishing.

Table I: Chemical compositions of alloys 600 and 690 (wt%)

	Ni	Cr	Fe	C	Si	Ti	Al	P	S
Alloy 600	75.80	15.45	6.98	0.055	0.48	0.18	0.171	0.005	0.001
Alloy 690	59.7	29.29	9.99	0.020	0.35	0.20	0.10	0.006	0.001

2.2 Immersion test

The specimens used to observe the microstructures of alloy 600 and 690 samples were prepared by chemical etching in a solution of 2 % bromine + 98 % methanol. The immersion test lasted for 10 and 100 hours under simulated PWR primary water conditions, i.e., 1200 ppm B (weight) and 2 ppm Li (weight) in pure water at 325 ℃ with a dissolved oxygen content of less than 5 ppb and a hydrogen content of 30 cm^3/kg H$_2$O. After the immersion test, the oxidized specimens were investigated using an optical microscope and SEM. The SEM examination was conducted using a JEOL JSM-IT100 (operating voltage 20 kV) and an FEI Sirion (operating voltage 10 kV).

3. Results and discussion

3.1 Microstructure of alloys 600 and 690

As shown in Fig. 1(a), needle-like particles precipitated inside of the grain boundaries and formed along the grain boundaries of the as-received alloy 600. On the other hand, intergranular precipitates were found in the as-received alloy 690, as shown in Fig. 1(b). It was discovered from a transmission electron microscopy (TEM) analysis that the intergranular and intragranular precipitates in the alloy 600 and 690 samples were Cr carbides. Figs. 1(c) and (d) show SEM images taken of the solution-annealed alloys 600 and 690, respectively. It was confirmed from the figures that the pre-existing Cr carbides (Figs. 1(a) and (b)) were completely dissolved by the solution-annealing treatments.
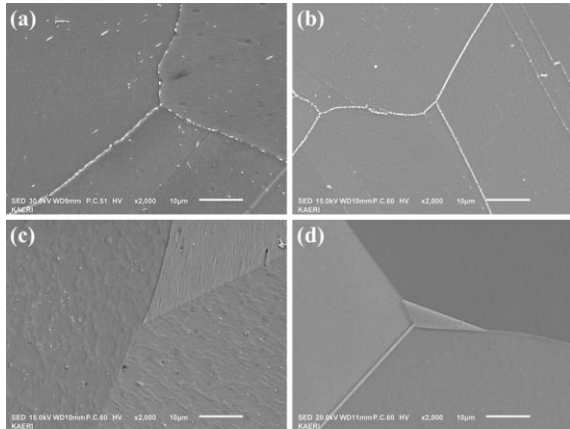
Fig. 1. Microstructures of the lloy 600 and 690 samples: (a) as-received alloy 600, (b) as-received alloy 690, (c) solution-annealed alloy 600 and (d) solution-annealed alloy 690

3.2 Surface morphology of the oxide

Fig. 2 shows the surface oxide morphologies depending on the surface conditions of the solution-annealed alloy 690 sample tested for 100 hours. As shown in the figures, different types of oxides were observed, and the filamentous oxides were most abundant on the ground specimens. They appeared in decreased amounts on the polished specimens and were rare on the chemically polished specimens [5]. The number density of the filamentous oxides also increased as the time was increased from 10 to 100 hours. Huang et al. [6] also found the filamentous oxides on the alloy 690TT in primary water at 325 ℃ and identified them as NiO. Thus the observed surface oxides in the present study, are considered as NiO, and were needed to be analyzed for the compositions and crystal structures using TEM.
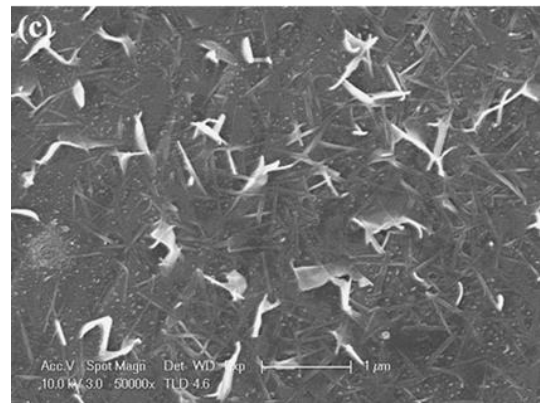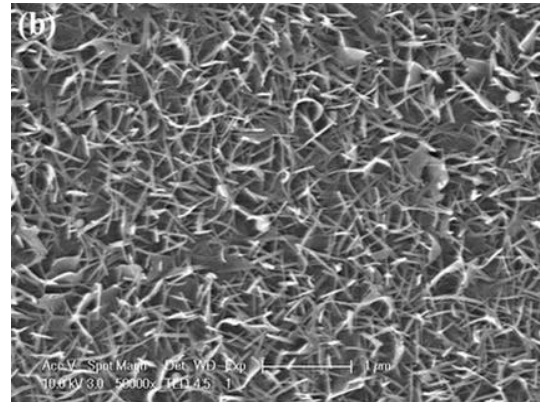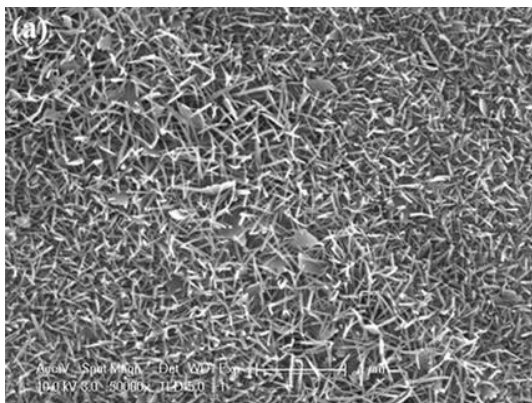

Fig. 2. Surface oxide morphology of solution-annealed alloy 690 samples after (a) grinding, (b) polishing and (c) chemical polishing

4. Conclusion

In the present study, surface oxides on solution-annealed alloys 600 and 690 tested at 325 ℃ in a simulated primary water environment were analyzed with optical microscope and SEM. The main objective was to observe the surface oxides depending on the surface conditions and the effects of surface oxidation on PWSCC. A rougher surface resulted in a denser oxide layer. It is considered that defects, dislocations and deformation layers on the rough surface react with oxygen to form an oxidation layer. An analysis by TEM appears to be necessary to identify the compositions and crystal structures of the oxides.

REFERENCES

[1] W. Bamford and J. Hall, A Review of Alloy 600 Cracking in Operating Nuclear Plants: Historical Experience and Future Trends, 11th Int. Conf. on Environmental Degradation of Materials in Nuclear Systems, Stevenson, WA, Aug. 10-14, 2003, pp. 1071-1081

[2] J. Panter, B. Viguier, J.-M. Cloué, M. Foucault, P. Combrade and E. Andrieu, Influence of oxide films on primary water stress corrosion cracking initiation of Alloy 600, J. Nucl. Mater. 348 (2006) 213–221.

[3] S.L Perez, D.W. Saxey, T. Yamada and T. Terachi, Atom-probe tomography characterization of the oxidation of stainless steel, Scripta Mater. 62 (2010) 855-858

[4] Y.S Lim, S.S Hwang and S.W Kim (2015), Surface oxidation Phenomena of Ni-Based Alloys in PWR Primary Water Environments. Proceedings of the KNS 2015 spring meeting, (pp. 1CD-ROM). Korea Republic of: KNS

[5] Yaolei Han, Jinna Mei, Qunjia Peng, En-Hou Han and Wei Ke, Effect of electropolishing on corrosion of Alloy 600 in high temperature water, Corrosion Science 98 (2015) 72-80

[6] Fa Huang, Jianqiu Wang, En-Hou Han and Wei Ke, Microstructural characteristics of the oxide films formed on Alloy 690TT in pure and primary water at 325 ℃, Corrosion Science 76 (2013) 52-59